

DESIGN EVALUATIONS OF THE NEW DOUBLE ROTOR INTERIOR PERMANENT MAGNET MACHINE

ARAVIND CV*, LAM PIN WEN

School of Engineering, Taylor's University, Taylor's Lakeside Campus,
No. 1 Jalan Taylor's, 47500, Subang Jaya, Selangor DE, Malaysia

*Corresponding Author: aravindcv@ieee.org

Abstract

Among various types of electric motor, permanent magnet motor is competent for high torque applications. Its torque producing point is resultant of air gap flux linkage between permanent magnet inbuilt in rotor and the stator winding. The reduction in air gap length improves the flux linkage, however it can only be reduced to a certain extent due to torque pulsation occurrence that increases cogging torque due to strong attraction of magnetic flux. A novel double rotor interior permanent magnet motor is proposed for improved torque performance. The key to this proposed structure is by introducing an additional outer rotor to the conventional permanent magnet motor. Consequently, this double rotor structure provides higher torque generation through an increase in torque producing point by utilising the flux linkage at stator yoke, meanwhile allowing the reduction of air gap length as the attraction of magnetic flux is distributed evenly from the inner and outer rotor. An electromagnetic analysis on the effect of torque producing capability to utilize the stator yoke flux is analysed using finite element method. An improvement of 22% of the motor constant square density value with an increase of 26% of average torque value in comparison than that of the conventional motor is reported in this paper.

Keywords: Double rotor, Air-gap flux linkage, IPM, Motor constant square density.

1. Introduction

Over the last years with technology advancement, electric motors being an important element for electromechanical energy conversion in industry [1, 2]. Electric motors are then continued to research to improve its torque for lower

Nomenclatures

F_m	Magneto-motive force
R_a	Air-gap reluctance, At/wb
L	Stack length, m
T	Electromagnetic torque developed, Nm
G	Motor constant square density, Nm/A/(w) ^{-1/2}
K_m	Motor constant
K_T	Torque constant
P	Power developed inside the machine
T_{avg}	Average torque, Nm

Greek Symbols

ϕ_s	Flux inside the single rotor, wb
ϕ_d	Flux inside the double rotor, wb
ϕ_s	Net flux, wb

power consumption especially for applications like Electric Vehicle (EV) [3, 4]. As a result, motor with higher torque generation draws lesser current from EV during transient state of acceleration and braking, allowing EV to travel for a further distance. In addition, with the recent development of permanent magnet, high air gap flux density can be obtained with the significant improved residual flux properties, thus permanent magnet motors have been a popular research topic nowadays to suit the modern technology needs. Double rotor permanent magnet motors however becoming a research topic for such applications and is expected to provide higher torque generation in comparison to the conventional Interior Permanent Magnet (IPM) motors. With the structure of double rotor motor to a vehicle, each rotor can operate individually to perform electronic differential to provide the required torque for each driving wheel and at different wheel speed [5].

The function of continuous variable transmission to power split can also be done with double rotor motors so that the internal combustion engine in hybrid electric vehicle can perform at narrow speed region to maximise the fuel efficiency [6]. Likewise double rotor motor is used for wind turbine to split the output power to obtain the optimal efficiency for wind energy harvesting [7].

In this paper, a novel Double Rotor Interior Permanent Magnet (DRIPM) motor is proposed for improve torque performance in comparison to the conventional IPM motor. As air gap flux linkage between the stator and rotor is the factor for torque production, maximising the air gap flux linkage in directly improves the motor torque performance [8, 9]. Thus the main objective is to improve the motor constant square density through an increase in torque producing capability of the proposed structure by maximising the air gap flux linkage around the stator core of an IPM motor. The mechanical and magnetic evaluation of the proposed DRIPM motor is compared to the conventional motor for the same sizing and volume.

2. Design Methodology

2.1. Design concepts

Figure 1 is the proposed DRIPM motor exploded view with the stator is made up with double header stator core of 24 poles with coil winding of star connection,

while the stator core is a T and I structure of stator laminations. The inner and outer rotor is made up with laminated rotor cores of 4 poles with each facing at the mutual axis. Each pole of the inner and outer rotors is inbuilt with permanent magnet of the same size and properties.

The double rotor structure gives an advantage to overcome the limitation of torque pulsation occurrence in conventional single rotor motor which constrains the minimum size of air gap length. As shown in Table 1 is the structural dimensions of DRFAPM motor. The theory of increasing the torque characteristic for motor reluctance through maximising the flux by double the rotor is presented in [10]. The design for both conventional and proposed motor are using the design guidelines presented in [11].

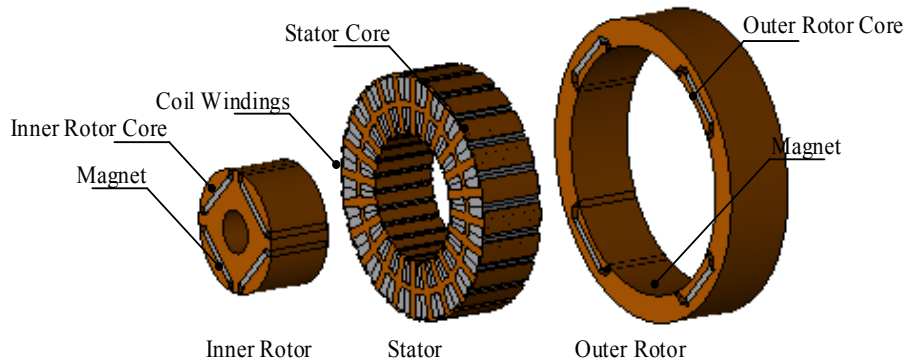


Fig. 1. Double rotor interior permanent magnet motor (exploded view).

2.2. Design principles

Permanent magnet motors operating principles is based on the power effects of magnetic circuit that tend to minimise the opposing magnetic flux lines of magnetic circuit [12]. It operates based on the interaction of magnetic field established by electromagnet of armature winding with that of the permanent magnet inbuilt at rotor [12]. The number of stator poles of the motor is divided evenly in three different phase for coil winding. When current injection to the motor in phase A, air gap flux linkage between stator and rotor is then generated to produce the torque. As torque is produced, the rotor starts to rotate to minimise the opposing magnetic flux lines of the magnetic circuit governed by Fleming's left hand rule [12]. Meanwhile when the opposing magnetic flux for phase A is at minimum, current is then injected to next phase for continuous rotation of the rotor. Saying so, the torque produced by a motor depends on the flux linkage on the air gap flux between the stator and rotor pole arc as shown in Fig. 2.

Fig. 3(a) shows the equivalent magnetic circuit of the conventional permanent magnet motor while Fig. 3(b) illustrates the circuit of the motor with double rotor. The selection design of the pole-arc is important since it is significant in influencing the torque producing capability by the motor. Reducing the air gap length between stator and rotor increase the magnetic flux linkage [8, 9]. On the contrary the properties of permanent magnet with strong attraction of flux results

in cogging torque especially when the motor is moving at a lower speed, thus there is a limit to the air gap length [13]. The relation of flux linkage (ϕ_s) of single rotor to air gap reluctance is presented in Eq. (2) below.

$$F_m = \phi_s R_a \tag{1}$$

$$\phi_s \propto \frac{1}{R_a} \tag{2}$$

where F_m is the Magneto Motive Force [$A-t$], R_a is the air gap reluctance [A/Wb].

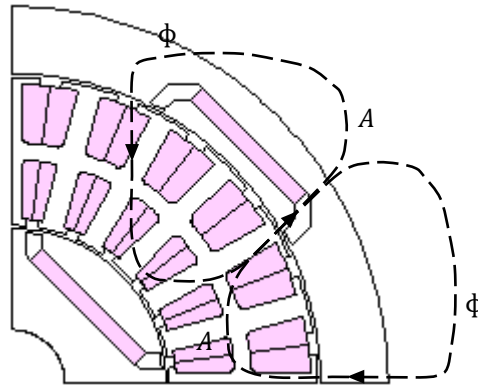


Fig. 2. Operating principles of DRFAPM motor.

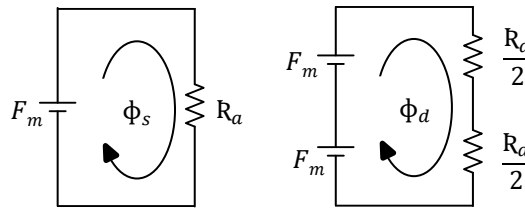


Fig. 3. Magnetic circuit, (a) single rotor and (b) double rotor.

To improve the torque performance of the motor, it can be done by either by optimising control circuit or to optimise the parameters of the motor especially the pole arcs. The motor is then introduced an outer rotor to the motor to overcome the torque pulsation factor which allow to reduce the air gap length of the motor [14]. The reduced air gap length not only minimises the reluctance contact flux linkage area, but the structure through dual air gap also double the torque producing point.

The introduction of the dual air gap increases the magneto motive force around twice that of the conventional motor. Therefore the relation of flux linkage (ϕ_d) over double rotor air gap reluctance is as in Eq. (4).

$$F_m + F_m = \phi_d \left(\frac{R_a}{2} + \frac{R_a}{2} \right) \quad (3)$$

$$\phi_d \propto \frac{2}{R_a} \quad (4)$$

The improvement in magnetic flux however will increase the torque of the motor to be proven by Eq. (5) as the torque is directly proportional to the square of magnetic flux.

$$T = \frac{1}{2} L \phi^2 \quad (5)$$

where T is torque [Nm] and L is the inductance [H].

3. Numerical Analysis

3.1. Finite element analysis (FEA)

Finite Element Analysis (FEA) tool is used to design and analysis of the motor constant square density as well to find the equivalent nodal force from distributed load force in stress analysis based on the numerical method [10]. To provide an accurate analysis for the motor design, an electromagnetic field analysis using finite element method is necessary. From the simulation, the direction of flux flow, magnetic flux density, and the torque performance of the motor are evaluated. As shown in Fig. 4 is the flux density of the proposed motor at different rotational angle position so that to maximise the air gap flux linkages by observing the flux flow. The motor is position at rotational angle of 0° , 7.5° , 15° , 22.5° , 30° , 37.5° respectively as shown from Fig. 4(a) to (f). In the analysis the effect due to mutual inductance is neglected. The lines around the motor indicate the flux saturation point and are evenly distributed among each quarter segment, thus allowing the motor to rotate freely at a slower rotational speed. As shown in Fig. 4(a), the flux saturated around stator of 45° , 135° , 225° and 315° as the position of permanent magnets. Likewise the saturated flux is aligned between the permanent magnets and the stator pole for Fig. 4(b) to (f) due to the attraction of magnetic flux, thus allowing the rotation of the rotors. The maximum flux density is 1.8 Tesla and is well below the property of the material used. However the limitations are on the static case and in dynamic would be experimentally tested in future, limiting to the non-linearity. For the core SS400 is used and the magnet used is NdFeB.

3.2. Evaluation parameters

For comparison on the level of performance for conventional and proposed structure, the methods of calculation Motor Constant Square Density G is used. The Motor Constant Square Density G is given as in Eq.(6).

$$G = \frac{(K_m)^2}{V} \quad (6)$$

where K_m is the machine constant in $[Nm/A/W^{-(1/2)}]$, V is the volume of the machine $[m^3]$. The machine constant can be further expressed as in Eq.(7).

$$K_m = \frac{K_T}{\sqrt{P}} \quad (7)$$

where K_T is the torque constant $[Nm/A]$ and P is the input power to the coil winding $[W]$. The torque constant is given as in Eq.(8).

$$K_T = \frac{T_{avg}}{I} \quad (8)$$

where T_{avg} is the fundamental torque $[Nm]$ and I is the maximum current input to the machine $[A]$.

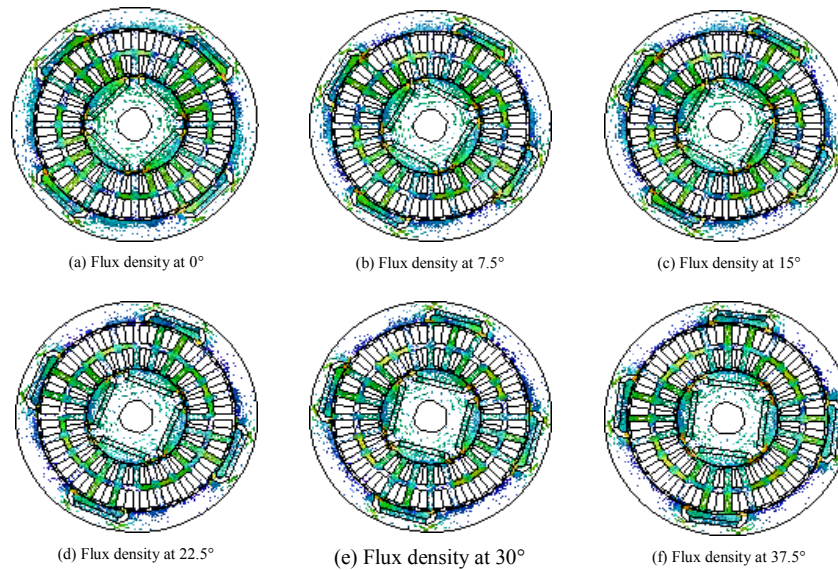


Fig. 4. Flux flow for various rotational angle.

4. Results and Discussions

4.1. Static characteristics

Figure 5 shows the average torque produced at no load when single phase current is injected at different phase angle from 0° to 90° with an interval of 10° in between. The analysis is operating at conditions with 5A rated current while its rotational speed is 1,800 rpm at frequency of 50 Hz. It can be observed that the torque is highest at the 10° where rotor starts to rotate from the original position with excitation from the single phase current magnetic flux. However as the rotor becomes unaligned with the excited stator the torque generated is reduced gradually. At phase angle 0° is considered as happy state as the air gap flux is not contributed to the torque due to excited stator is aligned with the position of permanent magnet.

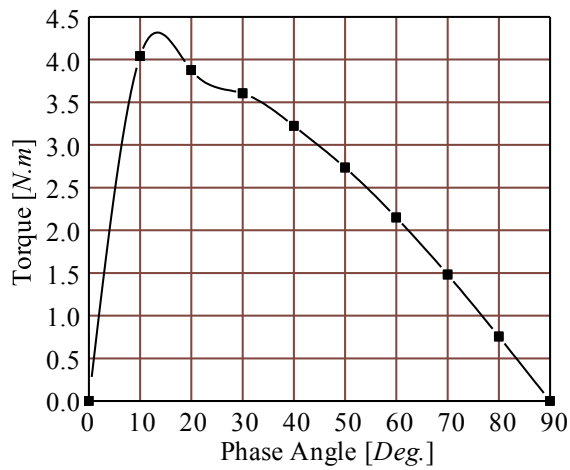


Fig. 5. Static characteristics.

4.2. Current characteristics

Figure 6 shows the static characteristics of DRFAPM for 2A, 3A, 4A, and 5A current. From the graph, the increase of excitation current increases torque producing capability of the motor. However there is a rated current for every motor depending on the thickness of coil winding that can withstand the amount of heat.

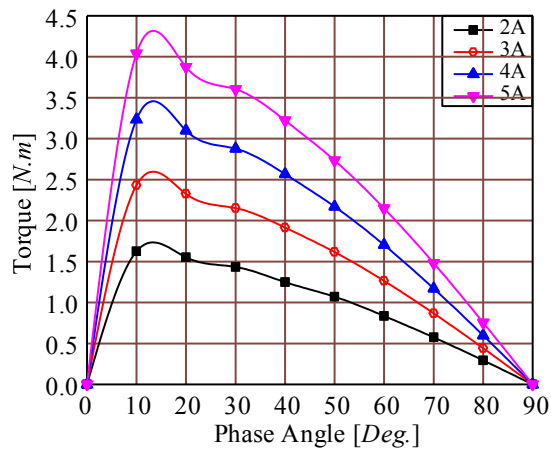


Fig. 6. Current torque characteristics.

4.3. Three phase torque characteristics

Figure 7 shows the torque generated when individual phase is excited sequentially. Each phase current is given an input of 5A but excited with a difference phase angle difference of 10° intervals. As shown in the graph, phase

A is excited at 0° until when it reaches phase angle of 10° , the next phase current B is excited, then followed by phase current C at 20° . The proposed DRIPM motor provides 26% more average torque in comparison to that of the IPM motor.

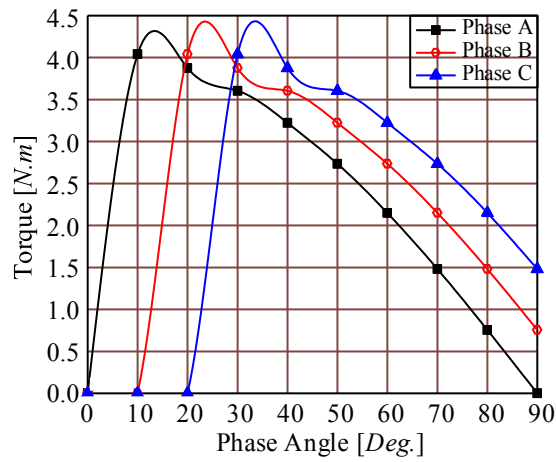


Fig. 7. Three phase static torque.

The sequential excitation loop will be repeating using appropriate control system method, thus generating complete excitation phase as shown in Fig. 8.

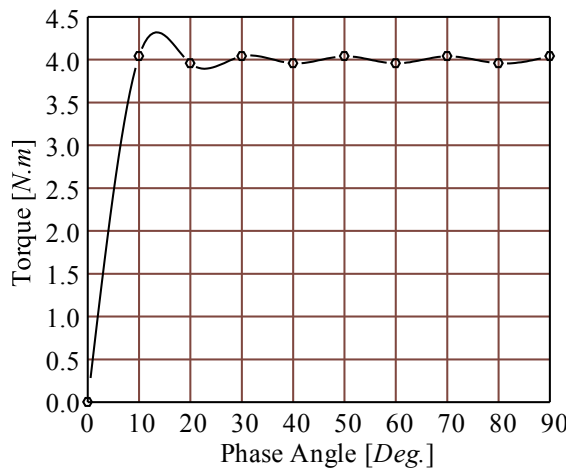


Fig. 8. Dynamic static torque.

4.4. Efficiency characteristics

Figure 9 shows the efficiency characteristics of DRFAPM motor. Under the conditions of 4A current amplitude at rotational speed 1800 rpm, the results indicate that DRFAPM motor obtains a maximum efficiency of 80.3% at phase

current of 0° . As the phase angle increases, the efficiency reduces with generated output torque as mentioned in results earlier. The efficiency of the motor however can be improved by reducing the losses, especially the main contribution from iron loss around the stator and joule loss from the coil winding.

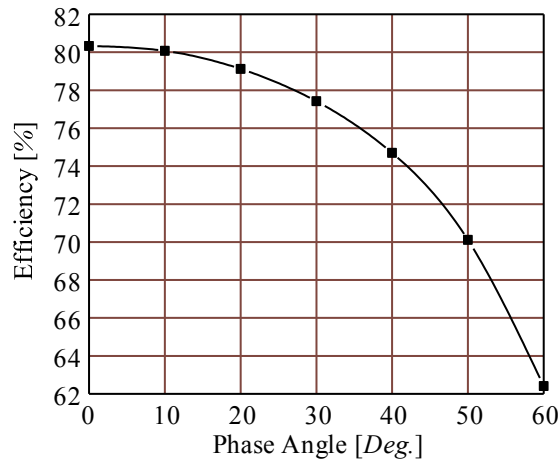


Fig. 9. Efficiency characteristics.

4.5. Comparative characteristics

Figure 10 is the comparison for IPM and DRFAPM motor for static and dynamic characteristics. Both motors are evaluated under the same sizing and parameters. Figure 10 shows that the static torque at maximum when injected current at optimal phase current. The result shows that DRFAPM motor and IPM motor provides highest torque of 4.043 Nm and 3.25 Nm at 10° and 20° respectively.

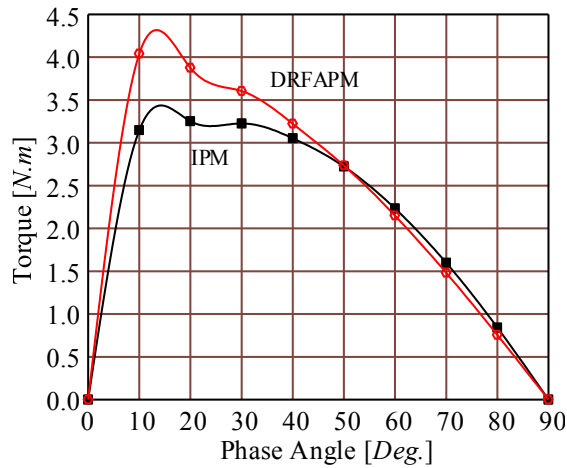


Fig. 10. Static characteristics.

Figure 11 is the load torque characteristics comparison for both motors. Both motor are operating at different rotational speed with correspondent to the frequency from 5 Hz to 60 Hz with interval of 5 Hz. The proposed DRFAPM motor provides an improvement of 22% of average torque with 3.61 Nm compared to the IPM motor with 2.94 Nm.

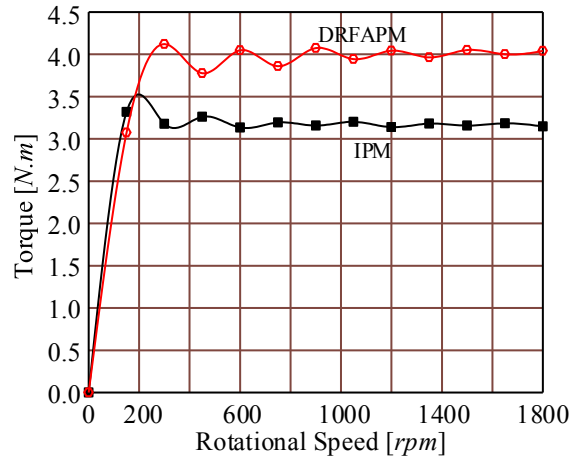


Fig. 11. Dynamic characteristics.

Table 1 shows the evaluation on IPM motor and DRFAPM motor torque characteristics. The table demonstrates the static characteristics value derived from the different current phase considering the motor constant square density.

Table 1. Comparison of motor constant square density.

Parameter		IPM	DRFAPM
I	[A]	5	5
V	[m ³]	5.99×10^{-4}	5.93×10^{-4}
T_{avg}	[Nm]	3.233	4.074
K_t	[Nm/A]	0.464	0.509
K_m	[Nm/A/W ^{-(1/2)}]	0.046	0.051
G	[Nm ² /A ² /W/m ³]	3.591	4.383

5. Conclusions

Double magnetic circuit can be realised using the double stator or through the double rotor circuit. Using the double rotor realisation the double rotor field assisted permanent magnet machine is proposed in this investigation. Static measurement characteristics of the double rotor flux assisted motor developed on the basis of increasing the air gap by proposing an outer rotor. The proposed DRFAPM motor provides an improvement of 22% for motor constant square density and 26% increment of average torque compared to the conventional IPM motor. These type of characteristics may find better in applications for low battery

powered electric vehicle. The drawback of this motor is that it produces high iron and joule loss due to the design structure of stator and coil winding located in the middle of the motor. For future work, it is recommend to use higher grade silicon steel with lower core loss characteristics for the laminated core.

References

1. Hyun, D.Y.; Markevich, E.; Salitra, G.; Sharon, D.; and Aurbach, D. (2014). On the challenge of developing advanced technologies for electrochemical energy storage and conversion. *Materials Today*, 17(3), 110-121.
2. Zhu, Z.Q.; and Howe, D. (2007). Electrical machines and drives for electric, hybrid and fuel cell vehicles. *Proceedings of IEEE*, 95(4), 746-765.
3. Ping, L.; and He-ping, L. (2011). Application of z-source inverter for permanent-magnet synchronous motor drive system for electric vehicles. *Procedia Engineering*, 15(1), 309-314.
4. Xu, P.; Hou, Z.; Guo, G.; Xu, G.; Cao, B.; and Liu, Z. (2011). Driving and control of torque for direct-wheel-driven electric vehicle with motors in serial. *Expert Systems with Applications*, 38(1), 80-86.
5. Kawamura, A.; Hoshi, N.; Kim, T.W.; Yokoyama, T.; and Kime, T. (1997). Analysis of anti-directional-twin-rotary motor drive characteristics for electric vehicles. *IEEE Transactions on Industrial Electronics*, 44(1), 64-70.
6. Hofman, T.; Steinbuch, M.; Van Druten, R.; and Serrarens, A.F.A. (2009). Design of CVT-based hybrid passenger cars. *IEEE Transactions on Vehicular Technology*, 58(2), 572-587.
7. Sun, X.; Cheng, M.; Hua, A.; and Xu, L. (2009). Optimal design of double-layer permanent magnet dual mechanical port machine for wind power application. *IEEE Transactions on Magnetic*, 45(10), 4613-4616.
8. Aravind, C.V.; Norhisam, M.; Mohammad, R.Z.; Ishak, A.; and Mohammad, H. M. (2012). Computation of electromagnetic torque in a double rotor switched reluctance motor using flux tube methods. *Energies*, 5(10), 4008-4026.
9. Aravind, C.V.; Norhisam, M.; Ishak, A.; Mohammad, H. M.; and Masami, N. (2013). Electromagnetic design and fem analysis of a novel dual air-gap reluctance machine. *Progress in Electromagnetics Research*, 140(1), 523-544.
10. Aravind, C.V.; Grace, I.; Rozita, T.; Rajparthiban, R.; Rajprasad, R.; Wong, Y.V. (2012). Universal computer aided design for electrical machines. *Proceedings of 8th International IEEE Colloquium on Signal Processing and its Applications*, 99-104.
11. Grace, I.; Teymourzadeh, R.; Bright, S.; and Aravind, C.V. (2011). Optimised toolbox for the design of rotary reluctance motors. *Proceedings of IEEE International Conference on Sustainable Utilization and Development in Engineering and Technology*, 1-6.
12. Krishnamurthy, M.; Fahimi, M.; and Edrington, B. (2005). Comparison of Various Converter Topologies for Bipolar Switched Reluctance Motor Drives. *Power Electronics Specialists Convergence*, 1858-1864.

13. Xu, H.Z.; and Ma, S. (2011). Research and simulation of permanent magnet synchronous motor based on coordination control technology. *Procedia Engineering*, 16(1), 157-162.
14. Aravind, C.V.; Norhisam, M.; Aris, I.; Ahmad, D.; and Nirei, M. (2011). Double rotor switched reluctance motors: fundamentals and magnetic circuit analysis. *IEEE Student Conference on Research and Development*, 294-299.